Nano Energy 126 (2024) 109582

Contents lists available at ScienceDirect

Nano Energy

journal homepage: www.elsevier.com/locate/nanoen

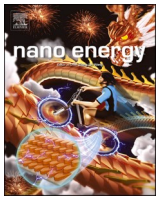

Communication

Interface defect formation for atomic layer deposition of SnO_2 on metal halide perovskites

Nitin Mallik [a,1], Javid Hajhemati [a,1], Mathieu Frégnaux [b], Damien Coutancier [a], Ashish Toby [a], Shan-Ting Zhang [c], Claudia Hartmann [d], Elif Hüsam [d], Ahmed Saleh [d], Thomas Vincent [c], Olivier Fournier [c,g], Regan G. Wilks [d], Damien Aureau [b], Roberto Félix [d], Nathanaelle Schneider [a], Marcus Bär [d,e,f], Philip Schulz [a,*]

[a] Institut Photovoltaïque d'Île-de-France (IPVF), UMR 9006, CNRS, Ecole Polytechnique - IP Paris, Chimie Paristech - PSL, Palaiseau, 91120, France
[b] Institut Lavoisier de Versailles, Université de Versailles Saint-Quentin-en-Yvelines, Université Paris-Saclay, CNRS, UMR 8180, Versailles Cedex 78035, France
[c] Institut Photovoltaïque d'Île-de-France, Palaiseau 91120, France
[d] Solar Energy Division, Helmholtz-Zentrum Berlin für Materialien und Energie GmbH (HZB), Berlin 12489, Germany
[e] Dept. X-ray Spectroscopy at Interfaces of Thin Films, Helmholtz-Institute Erlangen-Nürnberg for Renewable Energy (HI ERN), Berlin 12489, Germany
[f] Dept. of Chemistry and Pharmacy, Friedrich-Alexander-Universität Erlangen-Nürnberg (FAU), Erlangen 91058, Germany
[g] EDF R&D, IPVF, 91120 Palaiseau, France

ARTICLE INFO

Keywords:
Metal Halide Perovskite
Atomic Layer Deposition
Metal Oxide
ALD-SnO_2
Interface
Hard X-ray Photoelectron Spectroscopy

ABSTRACT

With the rapidly advancing perovskite solar cell (PSC) technology, dedicated interface engineering is critical for improving device stability. Atomic layer deposition (ALD) grown metal oxide films have drawn immense attention for the fabrication of stable PSC. Despite the advantages of ALD, the deposition of metal oxides directly on bare perovskite has so far not been achieved without damaging the perovskite layer underneath. In addition, the changes to the physicochemical and electronic properties at the perovskite interface upon exposure to the ALD precursors can alter the material and hence device functionality. Herein, we report on a synchrotron-based hard X-ray photoelectron spectroscopy (HAXPES) investigation of the interface between metal halide perovskite (MHP) absorber and ALD-SnO_2 electron transport layer. We find clear evidence for the formation of new chemical species (nitrogen compound, lead dihalides) and an upward band bending in the MHP and downward band bending in the SnO_2 towards the MHP/ALD-SnO_2 interface. The upward bending at the interface forms an electron barrier layer of ~400 meV, which is detrimental to the PSC performance. In addition, we assess the effectiveness of introducing a thin interlayer of the organic electron transport material Phenyl-C61-butyric acid methyl ester (PCBM) between MHP and ALD-SnO_2 to mitigate the effects of ALD deposition.

1. Introduction

In recent years, metal halide perovskite (MHP) solar cells have attracted immense attention among researchers due to the rapid advances in power conversion efficiency (PCE) beyond 26 %, which is now comparable to Si-based technologies [1,2]. Such extraordinary improvement of PCE in perovskite solar cells (PSCs) was made in light of the growing fundamental understanding of MHPs and improved interface engineering [3,4]. However, to this date, the long-term stability of PSCs, which is inherently affected by their interfaces, remains a key issue for widespread applications [5].

The intricacy of the involved interfaces owes to the perovskite material itself, which often includes five to six different elemental and molecular components, among them readily reduced metal cations, acidic organoammonium cations, and reactive halide species. [6] The charge transport layers (CTLs) that form a direct interface with the MHP are also critical to the stability of PSCs. [7] Comparing different CTLs, inorganic materials (e.g., metal oxides) have demonstrated better stability than organic materials in response to heat, light, and the local chemical environment. [8] Recent studies demonstrated that the stability of PSCs can be improved through deliberately tailoring interface properties and by introducing a compact metal oxide layer on the MHP.

* Correspondence to: CNRS, Institut Photovoltaïque d'Île de France (IPVF) – UMR 9006, IPVF, 18 Boulevard Thomas Gobert, Palaiseau 91120, France.
E-mail address: philip.schulz@cnrs.fr (P. Schulz).
[1] Nitin Mallik and Javid Hajhemati contributed equally to this work.

https://doi.org/10.1016/j.nanoen.2024.109582
Received 26 September 2023; Received in revised form 20 March 2024; Accepted 2 April 2024
Available online 8 April 2024

Several of these studies report on the incorporation of metal oxide CTLs (TiO_2, SnO_2, and NiO) in PSCs reaching PCE above 20 % [9–12].

The problems, in general, occur when the CTL is deposited directly on a bare MHP film, as this can potentially damage the absorber layer. Therefore, it is essential to choose a suitable deposition process to limit such damage. In a few demonstrations, oxide layers such as aluminum or titanium oxides were implemented directly on top of perovskite layers using spin coating, sputtering, thermal evaporation, and atomic layer deposition (ALD) [13,14]. Not all techniques are suited equally well; sputter deposition for instance usually damages the perovskite layer due to high energy ion bombardment [15]. Furthermore, the thermal instability of the perovskite materials limits the post-annealing temperature for the oxide growth when using spin coating and thermal evaporation [16].

In contrast, ALD is promising for growing oxide layers directly on top of MHP due to its relatively low deposition temperature, uniform coverage, and industrial scalability [17–19]. However, even this comparably "soft" deposition process can damage the MHP underneath due to the reliance of ALD on chemical precursors and reactions [20,21]. The reported PSCs, with ALD oxide deposited on top, have generally shown low PCEs in the range of 0.5 %-8.2 %. [22–29]

In a recent fundamental interface study of $Cs_{0.05}FA_{0.79}MA_{0.16}Pb-Br_{0.51}I_{2.49}$ MHP and ALD SnO_x, where FA and MA stand for formamidinium and methylammonium respectively, Hultqvist et al. observe the formation of additional chemical species involving Pb, Br, and N at the interface and suggest that this causes the formation of a barrier layer. [30] Aside from these select examples, there is a significant lack of fundamental research and hence understanding of the chemical interaction of the MHP surface with ALD precursors during the metal oxide preparation. In particular, its impact on the energy level alignment and hence electronic properties remains a key target for further investigation. These insights are, however, essential prerequisites for developing damage-free ALD metal oxide deposition processes for MHPs. Thus, they serve as the basis and motivation of this work.

In our study, we present a synchrotron-based hard X-ray photoelectron spectroscopy (HAXPES) interface study of $FA_{0.7}Cs_{0.3}Pb(I_{0.9}Br_{0.1})_3$ MHP with thin ALD SnO_2 overlayers (see Fig. 1) using two different photon energies (2 and 6 keV) for excitation that provide different information depths and hence assess the surface and interface properties, respectively. In this study we utilize a double cation mixed halide perovskite ($FA_{0.7}Cs_{0.3}Pb(I_{0.9}Br_{0.1})_3$) devoid of MA owing to its superior stability against thermal stress and moisture, rendering it better suited to withstand the ALD process [31]. The alloying of organic and inorganic cations has shown enhanced tolerance to heat, light and moisture (humidity up to 90 % RH) [32–34]. Our investigation yields evidence of chemical defects at the MHP/metal oxide interface due to reaction between MHP and ALD precursors with these chemical defects causing an upward band bending in the MHP that results in a barrier for electron

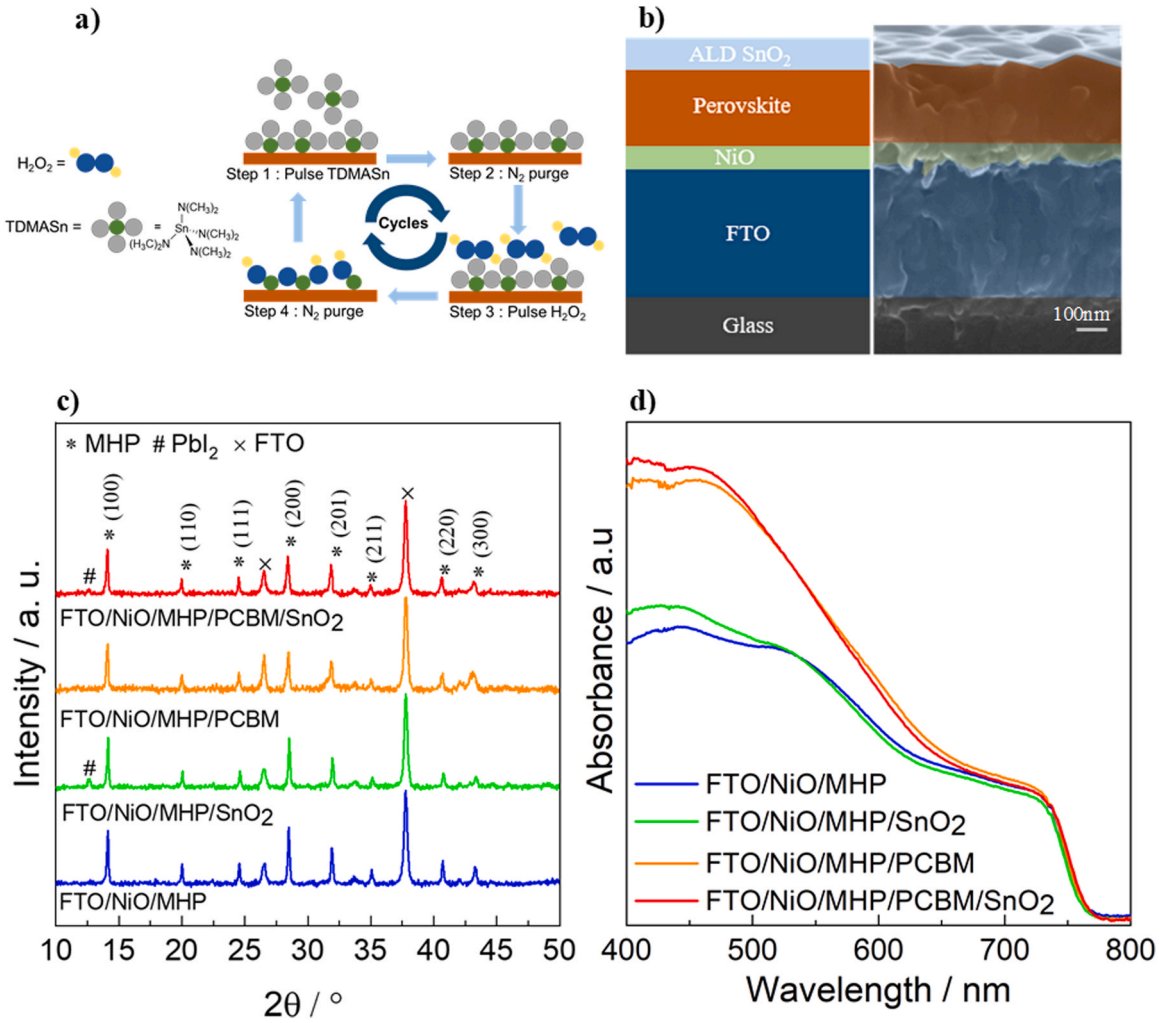

Fig. 1. (a) Simplified schematic of the ALD process with tetrakis(dimethylamido)tin(IV) (TDMASn) and H_2O_2 precursors to form SnO_2 layers. (b) Schematic of the investigated half-device stack of a P-I-N MHP based solar cell configuration without PCBM and corresponding cross-sectional SEM image. (c) XRD pattern of double cation MHP films with and without (PCBM/) ALD-SnO_2 top layers. (d) UV-Vis absorption spectra of samples with and without (PCBM/) ALD-SnO_2 top layers.

extraction at the MHP/SnO_2 interface. In an attempt to mitigate this, we also studied samples with Phenyl-C61-butyric acid methyl ester (PCBM) as an organic buffer layer between MHP and ALD SnO_2.

2. Results and discussion

The device architectures used in this interface study are comprised of F-doped tin oxide (FTO)-coated glass substrate, NiO,

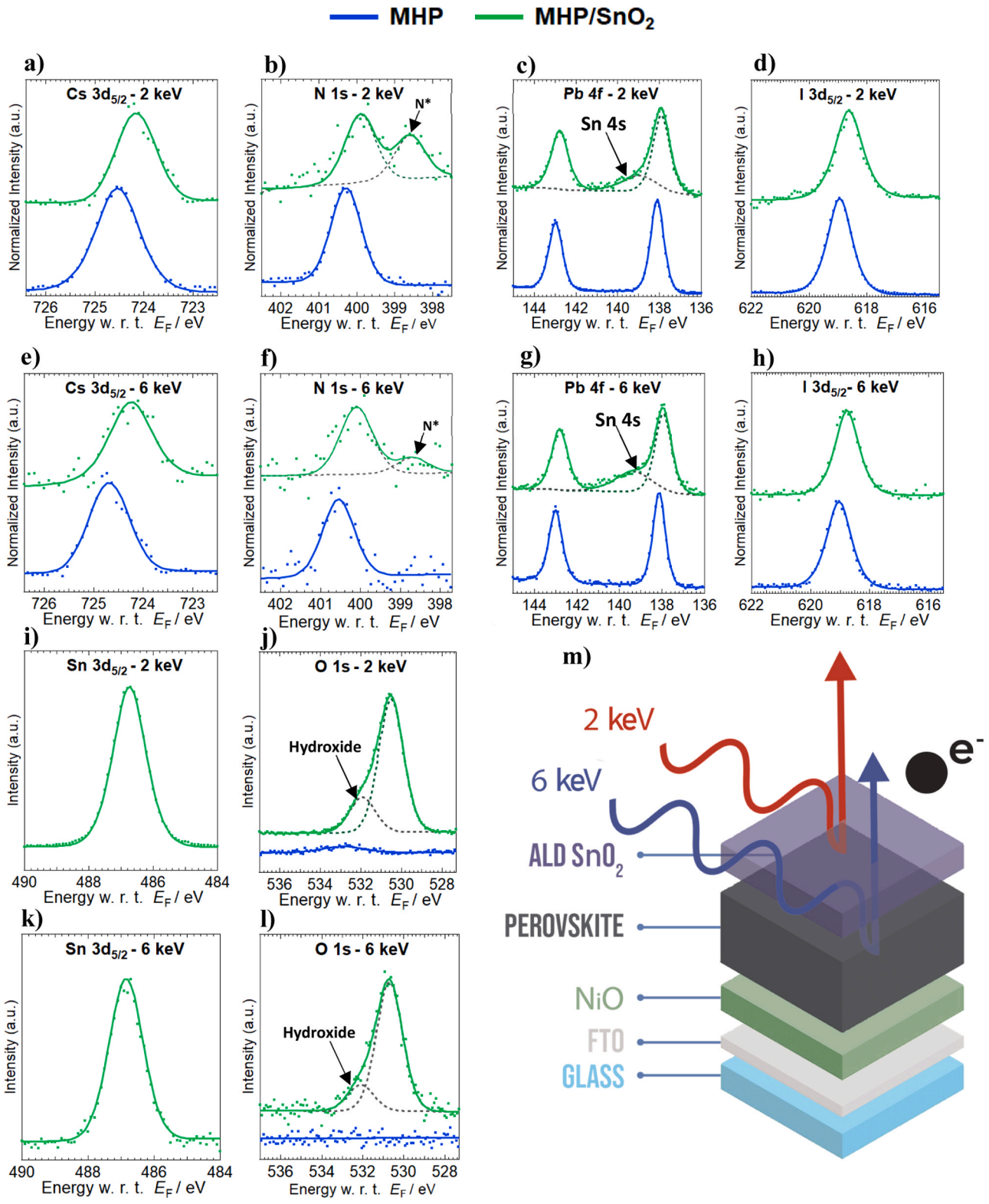

Fig. 2. (a-n) HAXPES high-resolution spectra (including fit analysis of some core levels) of Cs $3d_{5/2}$, N 1 s, Pb 4 f, I $3d_{5/2}$, Sn $3d_{5/2}$, and O 1 s of double cation MHP without (blue spectra) and with (green spectra) ALD SnO_2 top layers recorded using 2 and 6 keV excitation energy with Beryllium (Be) filter. N* indicates the peak component of a new nitrogen species as a reaction product of the ALD-SnO_2 deposition(o) Schematic of different probing depth of our HAXPES measurement using 2 keV and 6 keV photon energies.

$FA_{0.7}Cs_{0.3}Pb(I_{0.9}Br_{0.1})_3$ MHP with and without a 40 nm PCBM buffer layer, and ALD SnO_2 (see Fig. 1(b)). For this interface HAXPES study, 30 cycles of ALD SnO_2 are deposited on top of glass/FTO/NiO/MHP (/PCBM) samples (see Fig. 1(a) for a schematic presentation of the ALD cycles, see supporting information for more details). This corresponds to a 5 nm thick ALD SnO_2 film grown on a reference Si substrate in the same deposition run. However, note that the growth rates can differ for various substrates (see supporting information, S.I., Section 1.2).

Fig. 1(c) illustrates the X-ray diffraction (XRD) patterns of the bare MHP film, with ALD-SnO_2, PCBM, and PCBM/ALD-SnO_2 overlayers. Comparing the pattern of all samples, we observe a low-intensity PbI_2 peak at 12.5° for the samples with the ALD-SnO_2 layer on top. As this MHP is found to be thermally stable at 100 °C (see S.I., Figure S1), we attribute the formation of the PbI_2 peak to the chemical reaction between the MHP layer and the ALD precursors. Even the use of a protective PCBM interlayer does not fully inhibit this reaction (as indicated by the smaller but visible PbI_2 related peak in the corresponding X-ray diffraction pattern). The presence of PbI_2 is also observable in the absorbance spectra of the samples with ALD-SnO_2 as shown in Fig. 1(d) as a slight increase starting at a wavelength of around 515 nm (i.e., the band gap of PbI_2) and rising toward the UV-region [35]. We see that while the samples with ALD-SnO_2 present higher absorption in the wavelength range between 400 nm and 550 nm, the absorption becomes slightly lower for wavelengths longer than 550 nm. The samples containing a PCBM interlayer demonstrate increased absorption in the wavelength range between 400 and 650 nm, as indicated by the orange/red spectra, in contrast to the sample without a PCBM interlayer, represented by the green/blue spectra. We attribute this observation to the parasitic absorption in the PCBM film itself. The long-wavelength absorption onset at 750 nm is attributed to the fundamental absorption onset of the used double cation MHP.

The HAXPES spectra of the Cs $3d_{5/2}$, N 1 s, Pb 4 f, I 3d, Sn $3d_{5/2}$, and O 1 s core level regions of the bare MHP samples and after ALD SnO_2 deposition are depicted in Fig. 2. The intensities of the various MHP core levels are normalized to maximum intensity for better data visualization. The I 3d and Pb 4 f core level signals of pristine MHP show a minor shift in peak position (10–100 meV) between the data acquired for photon energies of 2 keV and 6 keV, respectively (see S.I.,Table S2). Considering the spectral resolution of our HAXPES experiment, we do not consider a shift of this order of magnitude to be significant.

The deposition of SnO_2 results in a larger shift of the lead and iodine core levels by approximately 200 and 300 meV to lower binding energies, respectively (see Fig. 3). These peak shifts are presumably indicating a change in electronic structure (i.e., band-bending), which can

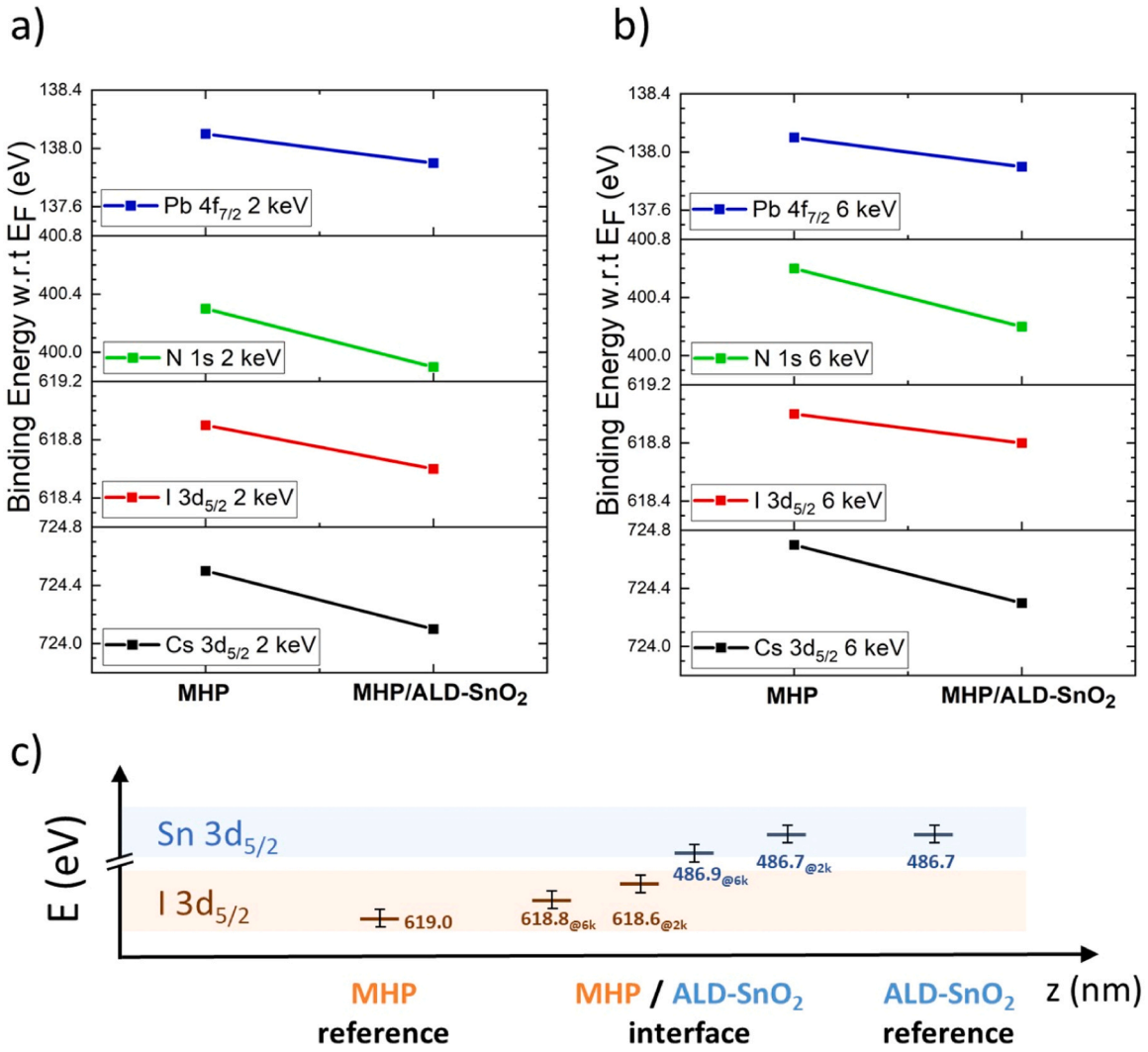

Fig. 3. Illustration of MHP core level shifts for MHP, MHP/ALD-SnO_2 (30 ALD Cycles) recorded at (a) 2 keV excitation energy (b) 6 keV excitation energy using the Be filter. (c) Schematic of I $3d_{5/2}$ and Sn $3d_{5/2}$ core level energies assessed at the MHP/SnO_2 interface. MHP and SnO_2 references are shown to the far left and right, respectively. All numbers are in eV with values estimated from HAXPES measurements performed at 2 keV photon energy labeled with a subscript @2k and those obtained at 6 keV photon energy labeled with a subscript @6k.

be caused by defect formation at the interface; notably this coincides with the formation of PbI_2 that we observed by XRD. We also monitored and compared the ratio of iodine to lead at the surface and subsurface of the perovskite layer before and after the ALD-SnO_2 deposition (see S.I., Table S4). The quantification shows that before SnO_2 deposition, the I/Pb ratio near the MHP surface is 2.7 i.e., almost equal to the expected stoichiometry value, decreasing to 2.4 with increasing probing depth. After SnO_2 deposition, we observed a more severe iodine deficiency and a contrary I/Pb profile, i.e., the deficiency is more apparent in the 2 keV measurements, in which the calculated I/Pb ratio is 0.7, i.e., almost one fourth of the initial stoichiometry ratio. In comparison, we find the ratio to be higher (1.7) in the more bulk-sensitive 6 keV measurements, indicating that this I depletion is driven by the interface formation with the SnO_2 or its synthesis process. Halide deficiency forms deep-level defects in the metal halide perovskite solar cells, which likely increases interfacial charge recombination and impede carrier extraction, negatively affecting PSCs performance. [36]

Upon SnO_2 deposition, a new peak appears at 138.9 and 139.2 eV (for 2 and 6 keV photon energy, respectively) in the Pb 4 f core-level spectra for the MHP/SnO_2 sample, which corresponds to the Sn 4 s core level. The shift in binding energy of Sn 4 s core level could be related to band bending in the SnO_2 film; however, the precision of the fit is significantly affected by the adjacent Pb 4 f core level fitting. Therefore, testing this hypothesis required further analysis of the Sn 3d and O 1 s core levels, as presented below.

However, first we closely inspect the N 1 s spectra, for which a new nitrogen peak is observed at 398.7 eV in case of the MHP sample with ALD-SnO_2. The relative intensity of this peak is higher at 2 keV excitation, indicating that the nitrogen species causing this N 1 s contribution is predominantly present within the ALD-SnO_2 layer or at the MHP/ALD-SnO_2 interface. Note that the corresponding peak intensity using 6 keV photon energy is close to the detection limit. The low photoionization cross-section (σ) at 6 keV (approximately 4 % of the respective value for 2 keV excitation see S.I., Table S1) resulted in a low signal-to-noise ratio for the N 1 s peak, precluding reliable peak quantification in that case. The formation of a new chemical state of the nitrogen species (N*) at the MHP interface would be consistent with an interfacial chemical reaction, as has been suggested before [30].

The emergence of the detected nitrogen species can be attributed to two potential origins: firstly, as a reaction/degradation product of the ALD precursor such as dimethylamine derivative, and secondly, as a degradation product arising from the formamidinium (FA) species present within the MHP structure. A plausible candidate for this degradation product is the *sym*-triazine, a nitrogen-containing heterocycle recognized as 1,2,5-triazine. [37,38] We note that the presence of *sym*-triazine at a FA-based halide perovskite/ALD-SnO_2 interfaces was further corroborated by another study using In-situ IR spectroscopy measurements. [39]

Furthermore, the N 1 s peak around 400 eV related to the FA species in MHP shifts by approximately 400–500 meV to lower binding energy after SnO_2 deposition, mostly in accordance with the I 3d and Pb 4 f core level shifts. The Cs $3d_{5/2}$ core level spectra exhibit a similar shift to lower binding energies. Hence, all MHP related core levels (e.g., Pb 4 f, I 3d, N 1 s, Cs $3d_{5/2}$) shift to lower binding energies upon ALD-SnO_2 deposition (see Fig. 3), providing evidence for an upward band bending in the MHP films towards the interface with the metal oxide overlayer.

We note that exposure to high-energy X-rays can induce damage to MHP samples, leading to inaccurate measurements of band bending [40]. To mitigate this issue, an aluminum (Al) filter was utilized to attenuate the 2 keV X-ray beam by a factor of 15 before it reached the sample to minimize the creation of defects that would shift the Fermi level and thereby impact band bending determination.

We analyzed the binding energy shift of the I $3d_{5/2}$ core level (measured on a fresh sample spot with the attenuated X-ray beam) as an indicator of the magnitude of band bending, which amounts to approximately 400 meV for both 2 keV and 6 keV photon energy (see S. I.; Table S3 and Figure S4). Assuming nearly flat band conditions at the MHP surface before interface formation, such an upward band bending corresponds to an interfacial electron extraction barrier. Of note, this result is further corroborated in the case of the MHP/SnO_2 samples, for which we observe a slightly broader I $3d_{5/2}$ peak for measurement with a full width at half maximum (FWHM) of 1.2 eV at 2 keV photon energy compared to the peak measured at 6 keV photon energy with a FWHM of 1 eV. This broadening suggests that we either capture multiple species with slightly different chemical shifts and band positions localized at the interface when the measurement is constrained to the interface region (2 keV), while the influence of these species is becoming negligible for the less surface-sensitive measurement (6 keV).

Next, we focus on the core levels of the SnO_2 film. The Sn $3d_{5/2}$ peak is located at 486.7 and 486.9 eV for 2 keV and 6 keV photon energy, respectively, corresponding to the Sn^{4+} state. [41] The shift in the binding energy of Sn $3d_{5/2}$ core level by 200 meV is similar to that observed for the Sn 4 s levels discussed above and indicates a slight downward band bending in the SnO_2 film towards the MHP/SnO_2 interface, which would favor the transport of electrons towards the presumably defect-rich interface and thus again negatively affected PSC performance.

For the MHP/SnO_2 samples, we see the presence of two O 1 s components using 2 keV and 6 keV photon energy. The O 1 s peak located at 530.7 eV when using 6 keV corresponds to the SnO_2 contribution, while the same peak is shifted to a lower binding energy of 530.5 eV when using 2 keV, corroborating band bending in the SnO_2 film. The signals at 531.9 eV and 532.1 eV seen in the spectra acquired at 2 keV and 6 keV photon energy, respectively, are attributed to the presence of hydroxides [22]. These residual by-products, such as hydroxides, are commonly observed in low-temperature ALD processes and can typically be eliminated by post-annealing treatment at temperatures around 150–200°C [42]. However, in this case, the low thermal stability of the MHP limits such post-heat treatment, as illustrated in Figure S1 (see S.I.). However, also the presence of "hydroxide" like species ascribed to surface adsorbates (particularly for the bare MHP sample) cannot be ruled out. This would be in line with the observation of one minor peak in the 2 keV data (blue line in Fig. 2j), while this peak is below the noise floor of the HAXPES measurements in the 6 keV data (Fig. 2 l).

Taken together, the shifts of the core level positions before and after deposition of the ALD layer, yield a qualitative picture of the possible band alignment between the MHP and SnO_2 film. For this purpose, we summarized the previously discussed core level positions of the elements in the MHP film measured at 2 keV and 6 keV photon energy in Figs. 3a and 3(b), respectively. In Fig. 3(c) we plot a schematic representation of the positions of the I $3d_{5/2}$ and Sn $3d_{5/2}$ core levels measured for the MHP/ALD-SnO_2 interface, which correspond to the signal from the MHP film and the ALD-SnO_2 film at the interface, respectively, with respect to the probing depth z. In this case, the core level data measured at 2 keV photon energy correspond to the signal originating from the region closer to the surface of the ALD-SnO_2 overlayer and the signal originating from the region of the MHP film that is closer to the interface. Conversely, the data measured at 6 keV photon energy correspond to the signal originating from the region of the ALD-SnO_2 layer closer to the interface, as well as from the buried region of the MHP film. We furthermore added the measured core level positions of the bare MHP surface and of a bare ALD-SnO_2 film deposited on a Si substrate as references to the far left and the far right of Fig. 3(c) as references, respectively. The data for the references including the associated

measured valence band onsets as well as energy level diagrams with the projected conduction band minima are included in the supplementary information (Figures S5 and S6).

If we assume flat band conditions in the unperturbed layers as well as negligible shifts and changes in the band gap due to the interfacial chemical reaction, then the changed core level positions after the interface formation can be interpreted as band bending in each layer. In this picture we observe, upward band bending in the MHP layer towards the defective interface, whereas we observe downward band bending in the SnO_2 layer towards this interface, which can be ascribed to the formation of a barrier for electron extraction. We note that even if we assume a deviation from flat band conditions for the initial perovskite surface, i.e. assuming that we have downward band bending in the perovskite, the interface formation would yield to lifting of this downward band bending equally detrimental for electron extraction.

For comparison the HAXPES results of the samples with PCBM buffer layer deposited on MHP film with and without ALD-SnO_2 overlayer are shown in Fig. 4. We use a 40 nm-thick PCBM interlayer in this experiment to protect the MHP from the potentially detrimental effect of the interface formation with ALD-SnO_2. Detecting signal from the buried MHP layer, as shown in Fig. 4, beneath the PCBM layer of nominal thickness of 40 nm is unexpected for the 2 keV-excited measurements (the inelastic mean free path, or IMFP, of the photoelectrons in question is approximately 4 nm at 2 keV and 11 nm for 6 keV excitation, see S.I., Section 1.3) and hence suggests for the presence of pinholes in the PCBM layer, which is confirmed by corresponding scanning electron microscopy images (see S.I., Figure S2 (c)). We use this opportunity to compare the MHP core level data of these samples before and after ALD deposition. Because MHP-related signal for these samples can be collected only through the area of the pinholes of the PCBM films, i.e., sample regions with overlayers insufficiently thick to completely attenuate photoelectron signals originating from the buried MHP absorber, the obtained spectra of MHP core levels exhibit markedly low signal-to-noise ratios. As the Pb 4 f and I 3d are the most prominent MHP-related lines, further data analysis is limited to spectra of these core levels. In addition, the absence of any discernible signal of the N 1 s core level is of particular interest. This observation holds significant implications, as it suggests that the observed additional nitrogen contribution in the MHP/ALD-SnO_2 sample is not a mere by-product of the ALD process but instead arises from interfacial chemical reactions specific to the deposition directly on top of the MHP without buffer layer (see S.I., Figure S8).

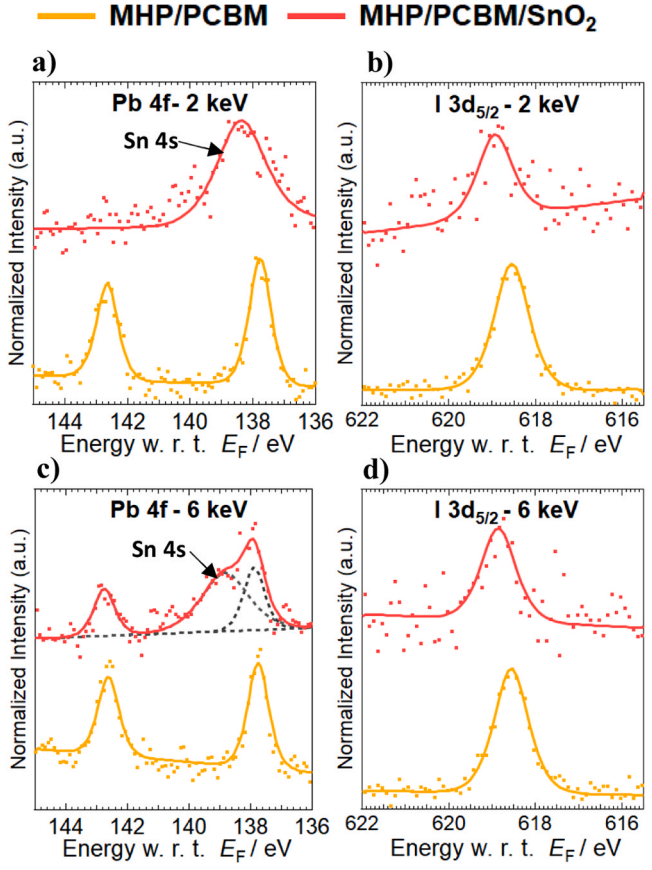

Fig. 4. HAXPES detail spectra of the Pb 4 f and I 3d core levels for the samples with double cation MHP/PCBM hetero-interfaces with and without SnO_2 top layers measured using 2 and 6 keV excitations with Be filter. Curve fit results are included.

After ALD SnO_2 deposition, the Pb 4 f core-level spectra do not exhibit any signature of Pb at 2 keV photon energy, indicating that the MHP layer is buried under a closed PCBM and ALD SnO_2 layers, or that pinholes are sufficiently small/few that the Pb 4 f signal, unlike the stronger I 3d, is not distinguishable from the background. Furthermore, this behavior indicates that iodine from the MHP might be migrating through the organic buffer layer towards the top interface. Here, as in Fig. 4(a), we observe the Sn 4 s peak at a binding energy of 138.2 eV. Whereas at 6 keV photon energy, we observe peaks corresponding to Pb 4 f core-level spectra. After the ALD process, the I 3d core levels shift by almost 400 meV and 300 meV to higher binding energy, compared to the MHP/PCBM reference, for the 2 keV- and 6 keV-excited spectra, respectively. The peak shift observed can be linked to the creation of even small amounts of donor states in the perovskite layer during the deposition process [43]. In comparison, the peaks corresponding to the Sn 3d and O 1 s core levels for 2 keV and 6 keV photon energy still show a small shift which suggests that downward band bending in the SnO_2 film, as observed previously in the MHP/SnO_2 sample, is not fully mitigated (see S.I., Figure S8).

The present study demonstrates that the PCBM buffer layer inadequately protects the MHP layer from exposure to ALD precursors, as evidenced by the existence of pinholes. This inadequacy exerts a detrimental impact on the overall performance of the device, as indicated in Table S5. Therefore, we modified the recipe for deposition of the PCBM film to improve the coverage for PSCs fabrication as shown in Figure S3 (e). In the modified recipe, the PCBM solution in chlorobenzene is heated to 60 °C prior to spin coating. The modified PCBM recipe is then incorporated to fabricate P-I-N PSCs (see S.I., Section 5 and Figure S9). In this improved configuration, the PCBM interlayer eventually led to an improvement of the device characteristics with notably improved open circuit voltages above 1 V, which however require further optimization to obtain high fill factor values.

To summarize, we found the formation of chemical defects at the MHP interface through HAXPES investigation. However, it remains unclear which ALD precursor (H_2O_2 or TDMASn) is the root cause of chemical defect formation. Therefore, in this section, we analyzed the impact of exposure to individual precursors, H_2O_2 and TDMASn, on the MHP and MHP/PCBM samples using lab-based XPS. Our objective was to determine which of the precursors caused interfacial reactions and defect formation. We focused on the N 1 s core level, as we had previously observed clear evidence of the formation of new species in the MHP/ALD-SnO_2 samples.

We exposed a silicon wafer to the TDMASn precursor to record the N 1 s position of the precursor, which served as a reference for comparison with the MHP and MHP/PCBM samples. The N 1 s peak originating from the TDMASn component was located at 401 eV on the silicon sample, as shown in Fig. 5(a). For the MHP sample, we did not observe any changes to the N 1 s core level even after exposure to 30 pulses of H_2O_2 precursor compared to the reference MHP sample. However, when exposed to 30 pulses of TDMASn precursor, we observed the formation of an additional peak attributed to the chemical reaction between MHP and TDMASn (see Fig. 5(b)).

For the PCBM reference and H_2O_2 exposed sample, we did not detect

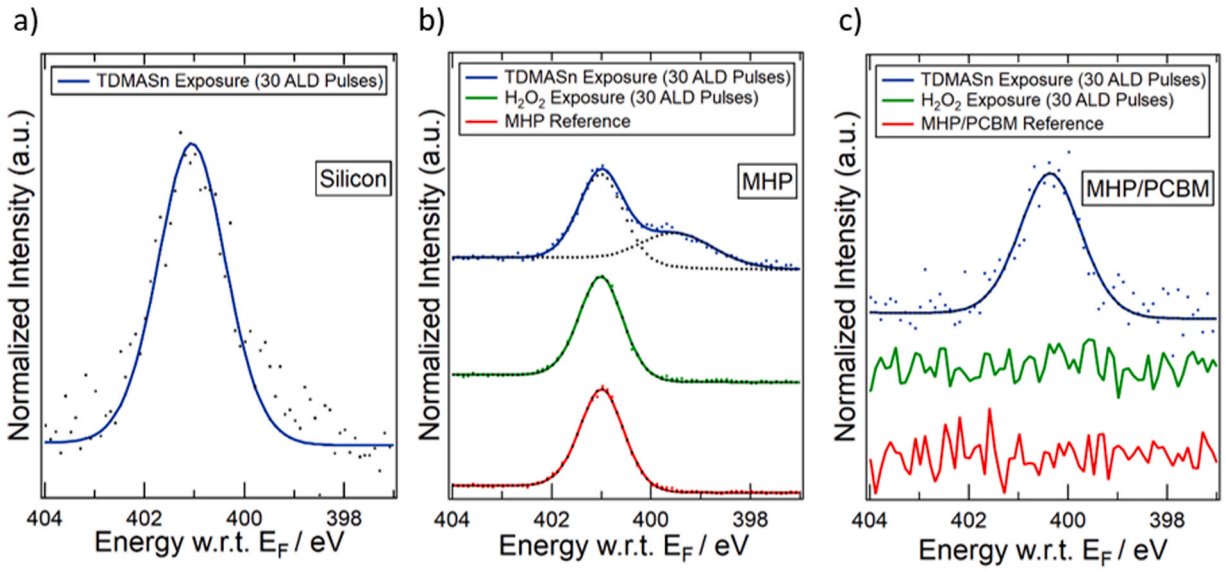

Fig. 5. XPS spectra (Al-K_α 1486.7 eV) of N 1 s core level of (a) Si wafer exposed to TDMASn precursor, (b) MHP and (c) MHP/PCBM spectra comparing f reference, H_2O_2 exposed and TDMASn exposed films.

any signal from MHP-FA species due to the thick PCBM film itself. Upon exposure to the TDMASn precursor, we observed the formation of a new peak attributable to the nitrogen contribution from the TDMASn precursor itself (see Fig. 5(c)). In summary, the exposure of TDMASn precursors on MHP caused interfacial reactions resulting in the formation of defective species. However, no evidence of such unwanted reaction was found upon exposure of H_2O_2 precursor.

Moving forward, one of the key challenges that requires immediate attention is the effective mitigation of surface damage encountered by MHP materials during their initial exposure to ALD metallic precursors. To address this issue, a promising avenue for exploration lies in the development of metalorganic precursors with reduced reactivity, aiming to minimize interfacial chemical reactions. Another intriguing possibility is the application of a suitable interlayer, such as two-dimensional (2D) perovskite or self-assembled molecules, between the MHP and ALD metal oxide films. The implementation of such interlayers presents a viable solution to shield the perovskite material from direct interaction with ALD precursors. These approaches hold significant potential in preserving the structural integrity and performance of MHPs and can ultimately contribute to the advancement and optimization of ALD processes for PSCs.

3. Conclusions

In summary, we report a synchrotron-based HAXPES interface investigation between MHP and ALD-SnO_2. This advanced characterization approach provided important information on the formation of new chemical species at the interface, i.e., a new nitrogen compound presumably from degraded formamidinium, as well as, lead dihalides. More in-depth analysis was performed to track the modification of band alignment induced by newly created interfacial defects. The Pb 4 f, I 3d, N 1 s, and Cs 3d core level peaks shifted to lower binding energy upon ALD-SnO_2 overlayer deposition; corresponding to an upward band bending inside the MHP at the interface, resulting in a significant electron barrier of over 400 meV and is therefore expected to negatively affect PCE performance of corresponding solar cells. Similarly, the observed downward band bending in the SnO_2 towards the interface is expected to limit PCE. The work is also extended to a system with a PCBM interlayer between MHP and SnO_2, which partly mitigates the chemical reaction when exposed to the ALD precursors. However, full protection against the degradation of the perovskite underneath is not achieved due to incomplete MHP coverage. In summary, this work acts as a guideline to explore alternative interlayers such as 2D perovskites or self-assembled organic molecules to chemically bind to the MHP species leading to a resilient protection against exposure to ALD precursors.

CRediT authorship contribution statement

Claudia Hartmann: Data curation, Investigation, Writing – review & editing. **Elif Hüsam:** Data curation, Investigation, Writing – review & editing. **Ashish Toby:** Formal analysis, Visualization, Writing – review & editing. **Marcus Bär:** Conceptualization, Formal analysis, Funding acquisition, Methodology, Project administration, Resources, Supervision, Validation, Writing – review & editing. **Shan-Ting Zhang:** Formal analysis, Writing – review & editing. **Philip Schulz:** Conceptualization, Data curation, Formal analysis, Funding acquisition, Methodology, Project administration, Resources, Supervision, Validation, Visualization, Writing – review & editing. **Mathieu Frégnaux:** Investigation, Methodology, Writing – review & editing. **Roberto Félix:** Investigation, Methodology, Supervision, Writing – review & editing, Data curation, Formal analysis. **Damien Coutancier:** Investigation, Writing – review & editing. **Nathanaelle Schneider:** Conceptualization, Methodology, Resources, Supervision, Validation, Writing – review & editing. **Nitin Mallik:** Conceptualization, Data curation, Formal analysis, Investigation, Methodology, Visualization, Writing – original draft, Writing – review & editing. **Javid Hajhemati:** Conceptualization, Data curation, Formal analysis, Investigation, Methodology, Visualization, Writing – original draft, Writing – review & editing. **Damien Aureau:** Investigation, Writing – review & editing. **Olivier Fournier:** Investigation, Writing – review & editing. **Regan G. Wilks:** Data curation, Formal analysis, Investigation, Methodology, Project administration, Supervision, Validation, Writing – review & editing. **Ahmed Saleh:** Investigation, Writing – review & editing. **Thomas Vincent:** Investigation, Writing – review & editing.

Declaration of Competing Interest

The authors declare the following financial interests/personal relationships which may be considered as potential competing interests: Philip Schulz reports financial support was provided by French National Research Agency.

Data Availability

Data will be made available on request.

Acknowledgments

This work was financially supported by the French Agence Nationale de la Recherche (ANR) with grant number: ANR-17-MPGA0012 and IPVF ANR-IEED-002-01. We thank Alexandre Blaizot for the SEM images. We thank HZB for the allocation of synchrotron radiation beamtime at BESSY II for HAXPES measurements.

Associated content

NA

Supporting Information

Experimental Methods; Thermal stability of $FA_{0.7}Cs_{0.3}Pb(I_{0.9}Br_{0.1})_3$ MHP; Morphology of Perovskite, PCBM, and ALD SnO_2; HAXPES data and graphs; P-I-N Solar cell performances.

Appendix A. Supporting information

Supplementary data associated with this article can be found in the online version at doi:10.1016/j.nanoen.2024.109582.

References

[1] H. Min, D.Y. Lee, J. Kim, G. Kim, K.S. Lee, J. Kim, M.J. Paik, Y.K. Kim, K.S. Kim, M. G. Kim, T.J. Shin, Perovskite solar cells with atomically coherent interlayers on SnO2 electrodes, Nature *598* (7881)) (2021) 444–450.
[2] N.J. Jeon, H. Na, E.H. Jung, T.Y. Yang, Y.G. Lee, G. Kim, H.W. Shin, S. Il Seok, J. Lee, J. Seo, A fluorene-terminated hole-transporting material for highly efficient and stable perovskite solar cells, Nat. Energy *3* (8) (2018) 682–689.
[3] P. Schulz, Interface design for metal halide perovskite solar cells, ACS Energy Lett. *3* (6) (2018) 1287–1293.
[4] M. Lira-Cantú, Perovskite solar cells: stability lies at interfaces, Nat. Energy *2* (7) (2017) 1–3.
[5] J.A. Christians, P. Schulz, J.S. Tinkham, T.H. Schloemer, S.P. Harvey, B.J. Tremolet de Villers, A. Sellinger, J.J. Berry, J.M. Luther, Tailored interfaces of unencapsulated perovskite solar cells for> 1,000 h operational stability, Nat. Energy *3* (1) (2018) 68–74.
[6] P. Schulz, D. Cahen, A. Kahn, Halide perovskites: is it all about the interfaces? Chem. Rev. *119* (5) (2019) 3349–3417.
[7] Q. Wang, N. Phung, D. Di Girolamo, P. Vivo, A. Abate, Enhancement in lifespan of halide perovskite solar cells, Energy Environ. Sci. *12* (3) (2019) 865–886.
[8] S.S. Shin, S.J. Lee, S.I. Seok, Metal oxide charge transport layers for efficient and stable perovskite solar cells, Adv. Funct. Mater. *29* (47) (2019) 1900455.
[9] Y. Lee, S. Lee, G. Seo, S. Paek, K.T. Cho, A.J. Huckaba, M. Calizzi, D.W. Choi, J. S. Park, D. Lee, H.J. Lee, Efficient planar perovskite solar cells using passivated tin oxide as an electron transport layer, Adv. Sci. *5* (6) (2018) 1800130.
[10] S. Jeong, S. Seo, H. Park, H. Shin, Atomic layer deposition of a SnO_2 electron-transporting layer for planar perovskite solar cells with a power conversion efficiency of 18.3%, Chem. Commun. *55* (17) (2019) 2433–2436.
[11] H. Wang, H. Liu, F. Ye, Z. Chen, J. Ma, J. Liang, X. Zheng, C. Tao, G. Fang, Hydrogen peroxide-modified SnO_2 as electron transport layer for perovskite solar cells with efficiency exceeding 22%, J. Power Sources *481* (2021) 229160.
[12] N. Ren, C. Zhu, R. Li, S. Mazumdar, C. Sun, B. Chen, Q. Xu, P. Wang, B. Shi, Q. Huang, S. Xu, 50°C low-temperature ALD SnO_2 driven by H_2O_2 for efficient perovskite and perovskite/silicon tandem solar cells. Appl. Phys. Lett. *121* (3) (2022).
[13] R.D. Raninga, R.A. Jagt, S. Béchu, T.N. Huq, W. Li, M. Nikolka, Y.H. Lin, M. Sun, Z. Li, W. Li, M. Bouttemy, Strong performance enhancement in lead-halide perovskite solar cells through rapid, atmospheric deposition of n-type buffer layer oxides, Nano Energy *75* (2020) 104946.
[14] F.J. Ramos, T. Maindron, S. Béchu, A. Rebai, M. Frégnaux, M. Bouttemy, J. Rousset, P. Schulz, N. Schneider, Versatile perovskite solar cell encapsulation by low-temperature ALD-Al_2O_3 with long-term stability improvement, Sustain. Energy Fuels *2* (11) (2018) 2468–2479.
[15] K.A. Bush, C.D. Bailie, Y. Chen, A.R. Bowring, W. Wang, W. Ma, T. Leijtens, F. Moghadam, M.D. McGehee, Thermal and environmental stability of semi-transparent perovskite solar cells for tandems enabled by a solution-processed nanoparticle buffer layer and sputtered ITO electrode, Adv. Mater. *28* (20) (2016) 3937–3943.
[16] Q. Wali, F.J. Iftikhar, M.E. Khan, A. Ullah, Y. Iqbal, R. Jose, Advances in stability of perovskite solar cells, Org. Electron. *78* (2020) 105590.
[17] Z. Xing, J. Xiao, T. Hu, X. Meng, D. Li, X. Hu, Y. Chen, Atomic layer deposition of metal oxides in perovskite solar cells: present and future, Small Methods *4* (12) (2020) 2000588.
[18] V. Zardetto, B.L. Williams, A. Perrotta, F. Di Giacomo, M.A. Verheijen, R. Andriessen, W.M.M. Kessels, M. Creatore, Atomic layer deposition for perovskite solar cells: research status, opportunities and challenges, Sustain. Energy Fuels *1* (1) (2017) 30–55.
[19] H. Wang, Y. Zhao, Z. Wang, Y. Liu, Z. Zhao, G. Xu, T.H. Han, J.W. Lee, C. Chen, D. Bao, Y. Huang, Hermetic seal for perovskite solar cells: An improved plasma enhanced atomic layer deposition encapsulation, Nano Energy 69 (2020) 104375.
[20] A.F. Palmstrom, J.A. Raiford, R. Prasanna, K.A. Bush, M. Sponseller, R. Cheacharoen, M.C. Minichetti, D.S. Bergsman, T. Leijtens, H.P. Wang, V. Bulović, Interfacial effects of tin oxide atomic layer deposition in metal halide perovskite photovoltaics, Adv. Energy Mater. *8* (23) (2018) 1800591.
[21] X. Dong, H. Hu, B. Lin, J. Ding, N. Yuan, The effect of ALD-Zno layers on the formation of $CH_3NH_3PbI_3$ with different perovskite precursors and sintering temperatures, Chem. Commun. *50* (92) (2014) 14405–14408.
[22] A.E. Bracesco, C.H. Burgess, A. Todinova, V. Zardetto, D. Koushik, W.M.E. Kessels, I. Dogan, C.H. Weijtens, S. Veenstra, R. Andriessen, M. Creatore, The chemistry and energetics of the interface between metal halide perovskite and atomic layer deposited metal oxides, J. Vac. Sci. Technol. A *38* (6) (2020).
[23] Y. Yang, Y. Zhang, L. Bai, D.M. Malouangou, J.T. Matondo, J. Pan, S. Dai, M. Cai, X. Liu, M. Guli, Research progress of atomic layer deposition technology to improve the long-term stability of perovskite solar cells, J. Mater. Chem. C. *10* (3) (2022) 819–839.
[24] H.H. Park, Inorganic materials by atomic layer deposition for perovskite solar cells, Nanomaterials *11* (1) (2021) 88.
[25] J.A. Raiford, S.T. Oyakhire, S.F. Bent, Applications of atomic layer deposition and chemical vapor deposition for perovskite solar cells, Energy Environ. Sci. *13* (7) (2020) 1997–2023.
[26] K.O. Brinkmann, T. Gahlmann, T. Riedl, Atomic layer deposition of functional layers in planar perovskite solar cells, Sol. RRL *4* (1) (2020) 1900332.
[27] S. Seo, S. Jeong, H. Park, H. Shin, N.G. Park, Atomic layer deposition for efficient and stable perovskite solar cells, Chem. Commun. *55* (17) (2019) 2403–2416.
[28] K. Deng, L. Li, Advances in the application of atomic layer deposition for organometal halide perovskite solar cells, Adv. Mater. Interfaces *3* (21) (2016) 1600505.
[29] J.A. Raiford, C. Chosy, B.A. Reeves, S.F. Bent, Tailoring the surface of metal halide perovskites to enable the atomic layer deposition of metal oxide contacts, ACS Appl. Energy Mater. *4* (9) (2021) 9871–9880.
[30] A. Hultqvist, T.J. Jacobsson, S. Svanström, M. Edoff, U.B. Cappel, H. Rensmo, E. M. Johansson, G. Boschloo, T. Törndahl, SnO_X atomic layer deposition on bare perovskite—an investigation of initial growth dynamics, interface chemistry, and solar cell performance, ACS Appl. Energy Mater. *4* (1) (2021) 510–522.
[31] C.C. Boyd, R. Cheacharoen, T. Leijtens, M.D. McGehee, Understanding degradation mechanisms and improving stability of perovskite photovoltaics, Chem. Rev. *119* (5) (2018) 3418–3451.
[32] Z. Li, M. Yang, J.S. Park, S.H. Wei, J.J. Berry, K. Zhu, Stabilizing perovskite structures by tuning tolerance factor: formation of formamidinium and cesium lead iodide solid-state alloys, Chem. Mater. 28 (1) (2016) 284–292.
[33] J.W. Lee, D.H. Kim, H.S. Kim, S.W. Seo, S.M. Cho, N.G. Park, Formamidinium and cesium hybridization for photo-and moisture-stable perovskite solar cell, Adv. Energy Mater. 5 (20) (2015) 1501310.
[34] C. Yi, J. Luo, S. Meloni, A. Boziki, N. Ashari-Astani, C. Grätzel, S.M. Zakeeruddin, U. Röthlisberger, M. Grätzel, Entropic stabilization of mixed A-cation ABX 3 metal halide perovskites for high performance perovskite solar cells, Energy Environ. Sci. 9 (2) (2016) 656–662.
[35] S.M. Jain, B. Philippe, E.M. Johansson, B.W. Park, H. Rensmo, T. Edvinsson, G. Boschloo, Vapor phase conversion of PbI_2 to $CH_3NH_3PbI_3$: spectroscopic evidence for formation of an intermediate phase, J. Mater. Chem. A *4* (7) (2016) 2630–2642.
[36] W.Q. Wu, P.N. Rudd, Z. Ni, C.H. Van Brackle, H. Wei, Q. Wang, B.R. Ecker, Y. Gao, J. Huang, Reducing surface halide deficiency for efficient and stable iodide-based perovskite solar cells, J. Am. Chem. Soc. *142* (8) (2020) 3989–3996.
[37] S. Thampy, B. Zhang, J.G. Park, K.H. Hong, J.W. Hsu, Bulk and interfacial decomposition of formamidinium iodide ($HC(NH_2)_2I$) in contact with metal oxide, Mater. Adv. *1* (9) (2020) 3349–3357.
[38] G.H. Gunasekar, K. Park, V. Ganesan, K. Lee, N.K. Kim, K.D. Jung, S. Yoon, A covalent triazine framework, functionalized with Ir/N-heterocyclic carbene sites, for the efficient hydrogenation of CO_2 to formate, Chem. Mater. *29* (16) (2017) 6740–6748.
[39] A.E. Bracesco, J.W.P. Jansen, H. Xue, V. Zardetto, G. Brocks, W.M. Kessels, S. Tao, M. Creatore, In Situ IR spectroscopy studies of atomic layer-deposited SnO2 on formamidinium-based lead halide perovskite. ACS Appl. Mater. Interfaces (2023).
[40] V. Milotti, S. Cacovich, D.R. Ceratti, D. Ory, J. Barichello, F. Matteocci, A. Di Carlo, P.M. Sheverdyaeva, P. Schulz, P. Moras, Degradation and self-healing of FAPbBr3 perovskite under soft-X-ray irradiation, Small Methods (2023) 2300222.

[41] J.F. Moulder, Handbook of X-ray Photoelectron Spectroscopy: A Reference Book of Standard Spectra for Identification and Interpretation of XPS Data, Physical Electronics Division. Perkin-Elmer Corporation, 1992, 978-0-9627026-2-4.
[42] J.W. Elam, D.A. Baker, A.J. Hryn, A.B. Martinson, M.J. Pellin, J.T. Hupp, Atomic layer deposition of tin oxide films using tetrakis (dimethylamino) tin, J. Vac. Sci. Technol. A *26* (2) (2008) 244–252.
[43] S.P. Dunfield, A. Bojar, S. Cacovich, M. Frégnaux, T. Klein, R. Bramante, F. Zhang, D. Regaldo, V. Dufoulon, J.B. Puel, G. Teeter, Carrier gradients and the role of charge selective contacts in lateral heterojunction all back contact perovskite solar cells, Cell Rep. Phys. Sci. *2* (8) (2021).

Nitin Mallik: Nitin Mallik received his Ph.D. (2023) from École Polytechnique, Institut Polytechnique de Paris, France. He obtained his B.S. degree in Materials Science from the Indian Institute of Science, Bengaluru, India in 2017. His research primarily focuses on the interlayer design of perovskite solar cells using atomic layer deposition (ALD) technique.

Javid Hajhemati: Javid Hajhemati is currently a postdoctoral researcher at CNRS (Centre National de la Recherche Scientifique), affiliated with Institut Photovoltaïque d'Ile-de-France (IPVF). He obtained his PhD in 2023 from Institut Polytechnique de Paris (IP Paris). His research focuses on designing and characterizing photovoltaic and semiconductor materials and devices, with particular emphasis on surface and interface analysis.

Mathieu Frégnaux: Mathieu Frégnaux is a Research Engineer at the French National Centre for Scientific Research (CNRS). He completed his PhD at the University of Lorraine (2009–2012), before working as a postdoctoral researcher at the University of Strasbourg (2013–2014) and the French Alternative Energies and Atomic Energy Commission – CEA-LETI (2014-2015). Since 2015, he is managing with Muriel Bouttemy the Center for Study and Training in Electron Spectroscopies (CEFS2) at the Lavoisier Institute of Versailles, equipped with 4 XPS, a SEM-FEG, a GD-OES and an Auger nanoprobe. His research interests include surface and interface science, photoemission, 2D materials, microelectronics and photovoltaics.

Ashish Toby: Ashish Toby is a Masters graduate from École Polytechnique, France in the field of Renewable Energy and a Bachelors graduate from the National Institute of Technology Calicut, India in the field of Mechanical Engineering.

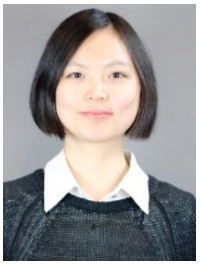

Shan-Ting Zhang: Dr. Shan-Ting Zhang is currently an Associate Researcher in Zhangjiang Laboratory. She received her Ph.D. (2017) from both Université Grenoble Alpes and Technical University of Darmstadt. She was postdoctoral fellow at National Centre for Scientific Research (CNRS) in France (2017-2020) and then worked as a researcher in IPVF (2020-2021). Her research interests include photovoltaic materials & devices (thin film & Si solar cells, module stability), and microelectronic semiconductor materials & devices (thin film transistors, compute-in-memory, high-k dielectrics).

Claudia Hartmann: Dr. Claudia Hartmann received her Diploma in physics from the Freie Universität Berlin in 2014 and her PhD degree in 2018 from Brandenburg Technical University Cottbus-Senftenberg (BTU). She joined the Young Investigator Group – Interface Design at HZB, headed by Dr. Marcus Bär, as a PhD student in 2014 and from 2018 to 2021 as a Post-doctoral researcher, studying metal halide perovskite used for solar cells and their surfaces/interfaces using photoelectron spectroscopy. She has (co)authored 17 publications and has presented her research at 4 international conferences.

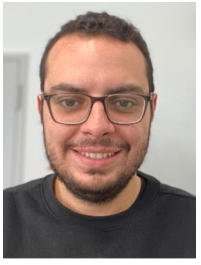

Ahmed Saleh: Ahmed Saleh is working as a Ph.D. student at Helmholtz-Zentrum Berlin in Germany. Previously he obtained his M.S. in Physics from Stuttgart University (2021) and his B.S. in Nanoscience (major) and Nanophysics (minor) form Zewail University in Egypt (2017).

Olivier Fournier: Olivier Fournier got a PhD in Physico-chemistry in 2021 from PSL (Paris Sciences Lettres) university and ENSCP (Ecole Nationale Supérieure de Chimie de Paris). His research at the Institut Photovoltaïque d'Ile-de-France (IPVF) focused on the study of interfaces in perovskite solar cell, specifically between the perovskite and ALD-grown materials. After a postdoc on advanced optical characterization of semitransparent perovskite solar cells at IPVF, he changed path and joined the Microfluidics Innovation Center as research engineer. His current work focuses on the development of technical solutions for microfluidics applied to biology, in the framework of collaborative research projects.

Damien Aureau: After his diploma in chemistry, Damien Aureau became doctor of Physics of Polytechnique school in 2008. In his career, he worked in several laboratory in the world, the IMTA in Mexico, the University of Turku in Finland, the Helmholtz Zentrum in Berlin, the University of Cork in Ireland and the University of Texas at Dallas. He is now working as a permanent researcher for the CNRS in the Lavoisier Institute in the University of Versailles, in the "electrochemistry and physical-chemistry of surfaces" group. His field of expertise focuses into the field of surface modification and reactivity of various materials. He was a laureate of the EMERGENCE project (INC-CNRS) aimed to develop a new field of research on 2D-Materials. He is a specialist of the different techniques used to study these surfaces and interfaces, especially in photoemission spectroscopies.

Nathanaelle Schneider: Nathanaelle Schneider is a CNRS (Centre National de la Recherche Scientifique) Researcher in the laboratory of the Institut Photovoltaïque d'Ile-de-France (IPVF). She was recruited in 2013 after a PhD in Chemistry at Heidelberg and Strasbourg universities (summa cum laude distinction). Her research is focused on the synthesis of new functional materials by ALD (Atomic Layer Deposition) for photovoltaic applications. Using contributions of organometallic chemistry, in-situ characterization, surface science, it has led to new methodological approaches for the design of ALD precursors, material solutions for photovoltaic devices and new functional materials. In 2020, she was awarded the CNRS bronze medal.

Philip Schulz: Philip Schulz holds the position of Research Director at the Centre National de la Recherche Scientifique (CNRS) and pursues his research activities at the Institut Photovoltaïque d'Île-de-France (IPVF). At IPVF, he serves as the co-head of the Characterization, Modelling and Reliability program, and leads the Interfaces and Hybrid Materials group founded via a Young Investigator award in the "Make Our Planet Great Again" initiative of President Emmanuel Macron of the French Republic. His research activities comprise the design and analysis of interfaces in emerging functional optoelectronic materials with a focus on their use in energy applications.